The Heisenberg model on the 1/5-depleted square lattice and the CaV_4O_9 compound

L. O. Manuel, M. I. Micheletti, A. E. Trumper, and H. A. Ceccatto
Instituto de Física Rosario, Consejo Nacional de Investigaciones Científicas y Técnicas and Universidad Nacional de Rosario, Bvd. 27 de Febrero 210 Bis, 2000 Rosario, República Argentina

We investigate the ground state structure of the Heisenberg model on the 1/5-depleted square lattice for arbitrary values of the first- and second-neighbor exchange couplings. By using a mean-field Schwinger-boson approach we present a unified description of the rich ground-state phase diagram, which includes the plaquette and dimer resonant-valence-bond phases, long- and short-range Néel orders, an incommensurate phase and other magnetic orders with complex magnetic unit cells. We also discuss some implications of our results for the experimental realization of this model in the CaV_4O_9 compound.

The CaV_4O_9 is the first example of a quasi two dimensional magnetic system with a spin gap.[1] As such, it has received much attention recently, with a large part of this activity devoted to understanding the mechanism of the gap formation.[2−17] Most of these works have considered the Heisenberg model on the so called CAVO lattice, *i.e.*, the 1/5-depleted square lattice of Fig. 1, with both first- and second-neighbor interactions (Following the notation in Ref. 3, we will call J_1 and J_1' to the nearest-neighbor intra and interplaquette couplings respectively, and, accordingly, J_2 and J_2' for the second-neighbor interactions).

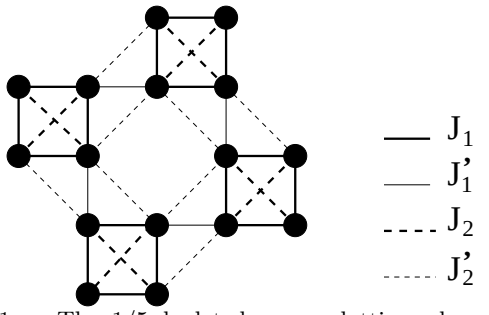

FIG. 1. The 1/5-depleted square lattice, also called a CAVO lattice. We indicate also the first- and second-neighbor exchange couplings between vanadium atoms in the CaV_4O_9 compound.

A variety of methods, including quantum Monte Carlo,[2,4] perturbative and high-temperature series expansions,[3] exact diagonalization,[5] different mean-field approximations,[6–8], renormalization group methods[9], and other techniques[10,11], have been applied to this model, leading to the conviction that it has a spin gap for $J_1 \gtrsim J_1'$ and/or large enough frustrating second-neighbor interactions. Based on simple considerations, most authors have assumed $J_1' \approx J_1$, $J_2' \approx J_2$ and $J_2 \approx 0.5J_1$, and, to lowest order, identified the gap as the singlet-triplet gap above the plaquette resonant-valence bond (PRVB) state obtained from the four nearest-neighbor V atoms coupled by J_1.[6] However, by using LDA calculations Pickett[12] concluded that the second-neighbor interactions might be dominant, with $J_2 \approx 2J_1$. In this case the singlet ground state would correspond to weakly-coupled metaplaquettes formed by V atoms connected by the J_2' bonds. On the other hand, from the analysis of neutron inelastic scattering data Kodama *et al.*[13] estimated $J_2 \approx 0.1J_2'$, $J_1' \approx J_1 \approx 0.4J_2'$ in order to reproduce the dispersion of the lowest triplet excitation. Moreover, other authors have suggested that the exchange couplings could be temperature dependent due to spin-phonon interactions.[8]

All the above mentioned works assumed that a single non-degenerate orbital on V atoms is occupied. Marini and Khomskii[14] argued, however, that orbital ordering and associated structural distortions determine the magnetic properties of the vanadates CaV_nO_{2n+1}, and proposed a structure of weakly-coupled dimers along J_1' bonds for the ground state of CaV_4O_9. Recent work by Gelfand and Singh[15] concluded that this proposal is not consistent with experimental observations, and that the PRVB and metaplaquettes scenarios are both able to produce a reasonable explanation for the observed gap and uniform susceptibility. In a very recent work,[16] Katoh and Imada pointed out serious limitations of the simple single-orbital model to reproduce results from neutron inelastic scattering. They partially solved these discrepancies between theoretical predictions and experimental observations by considering the effects of orbital degeneracy and orbital order, which lead to an effective spin Hamiltonian with exchange couplings strongly dependent on patterns of orbital occupancy.

The above brief summary of previous work on CaV_4O_9 points to the difficulties found to determine the real values of the competing couplings involved. Consequently, it seems worth to us the investigation of the general ground-state structure of the quantum Heisenberg antiferromagnet on the CAVO lattice for arbitrary values of J_1, J_1' and J_2 (we take $J_2' = J_2$ for simplicity), in order to identify possible phases with the properties observed experimentally. We report here the results of such an investigation, which is based on the use of the mean-field Schwinger boson approximation.

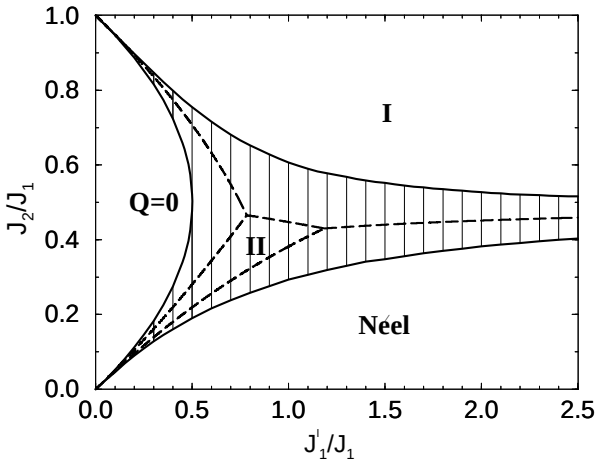

FIG. 2. Ground-state structure of the classical Heisenberg model on the CAVO lattice. Full lines indicate the stability regions of phases I, Néel and $Q = 0$. In the shaded area an incommensurate phase is stabilized in the thermodynamic limit. The dashed lines indicates the stable phases I, II, Néel and $Q = 0$ for a cluster of 32 spins.

Let us start by considering first the ground state of the classical Heisenberg model on the lattice of Fig. 1. A standard analysis[17] shows that even in this case the model turns out to be very rich, as shown in Fig. 2. The stability regions of the different phases are indicated by full lines; we also show, for further use, the stable phases in lattices of up to 32 spins (dashed lines). The $Q = 0$ and Néel phases have antiferromagnetic order in the plaquettes which repeats itself along the translation vectors $\delta_1 = (2, 1)a$, $\delta_2 = (-1, 2)a$ with magnetic wavevectors $\mathbf{Q} = (0, 0)$ and $\mathbf{Q} = (\pi, \pi)$ respectively (a is the nearest neighbor V-V distance). Phases I and II have both a 8-spin magnetic unit cell, translation vectors $\delta_1 = (1, 3)a$, $\delta_2 = (-3, 1)a$ and a magnetic wavevector $\mathbf{Q} = (\pi, \pi)$, with the corresponding spin arrangements in the unit cells shown in Fig. 3a,b. The angle φ verifies $\tan\varphi = -J_1'/2J_2'$ in phase I and $\tan\varphi = -2J_1/J_1'$ in phase II. Finally, the shaded area is the stability region of an incommensurate phase very difficult to characterize. This makes the consideration of the quantum nature of the spins quite involved in this phase (see below).

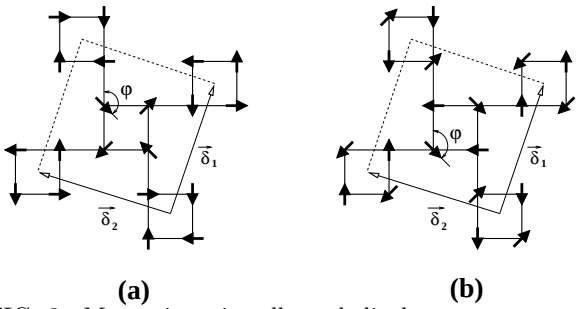

FIG. 3. Magnetic unit cells and displacement vectors δ_1 and δ_2 corresponding to a) Phase I and b) Phase II (see main text).

We must now correct the classical diagram of Fig. 2 by introducing the effects of quantum fluctuations. In order to do so, we will use the mean-field Schwinger boson theory[18], which has already been applied to the CAVO lattice without frustrating second-neighbor interactions.[7] This approach is suitable for the problem at hand since it allows to treat magnetic and non-magnetic quantum phases in an unified way. Moreover, despite the fact that the Schwinger boson theory is known to overestimate the stability of magnetic phases, it most often provides a qualitatively reliable phase structure. On the other hand, its predictions can be systematically corrected by the inclusion of fluctuations in the mean-field order parameters,[19] which has been shown to bring Schwinger boson results well in line with exact values on finite lattices and with the predictions of other more accurate methods in the thermodynamic limit.

Using the standard representation of spin operators in terms of two boson fields linked by the local boson number restrictions, quantum corrections to the phase diagram of Fig. 2 can be obtained by simply choosing the right initial structure of the order parameters in solving the self-consistent equations.[20] Although this is a matter of a straightforward energy minimization, the large number of spins in the magnetic Brillouin zone makes the calculations involved and computationally demanding. In addition, since we have no simple characterization of the incommensurate phase, in this region we had to rely on an extensive search for global solutions of the minimization equations. The strategy used was first to determine the classical ground state in clusters of up to 64 spins, and then searching for the absolute energy minimum in the quantum incommensurate phase starting from these large magnetic cells. In particular, up to 32 spins the stable classical phases are those showed in Fig. 2 with dashed lines. In addition to the commensurate phases above described, there is another phase stable only along the dashed line that separates phases I and II; it has a 4-spin magnetic cell and magnetic wavevector $\mathbf{Q} = (0, \pi)$. This classical phase is particularly interesting as a starting point for the search of order parameters in the quantum incommensurate phase. This is so because no pair of classical vectors in the magnetic motif are collinear or anticollinear, which means that the ferromagnetic and antiferromagnetic channels are both active in the minimization. Furthermore, for clusters with more than 32 spins the resulting classical stable phases are incommensurate (span the cluster). We stress that this investigation of the incommensurate phase is allowed only because of the particular properties of the Schwinger boson theory, since other semiclassical approaches (spin wave theory, for instance) require the precise knowledge of the classical ground-state structure. Moreover, the inclusion of quantum (non-magnetic) phases in the diagram of Fig. 2 is possible because the Schwinger bosons preserve the rotational invariance of the Heisenberg Hamiltonian when there is no condensation (magnetization) in the system.

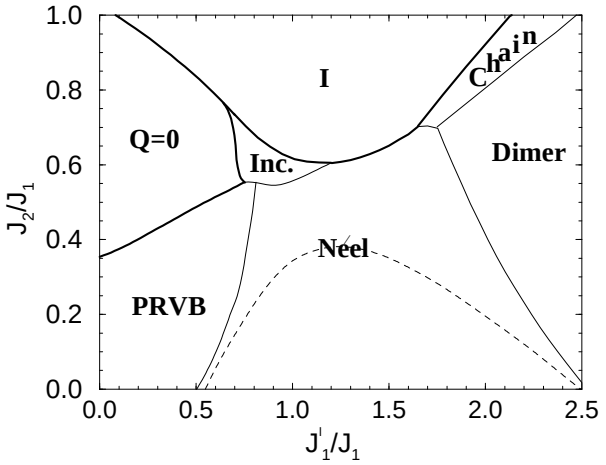

FIG. 4. Ground-state structure of the quantum Heisenberg model on the CAVO lattice. Full thick(thin) lines indicate first(second)-order phase transitions; the dashed line separates long-range and short-range Néel orders. See main text for a description of the different phases.

After the consideration of quantum fluctuations at mean-field order, the ground state has the complex structure shown in Fig. 4. The $Q = 0$-PRVB transition is weak first order, while the incommensurate-short-range Néel transition might be a very weak one instead of the second-order transition indicated. The Chain phase corresponds to disconnected zig-zag chains along $J_1'$and J_2 bonds, with short-range antiferromagnetic correlations between nearest-neighbor spins in the chains (this phase is essentially the ground state proposed by Marini and Khomskii[14]). The PRVB and dimer phases are the standard singlet phases discussed in previous works, consisting respectively of isolated plaquettes made up by J_1 bonds and the J_1' dimer covering. For $J_2' \gg J_1'$ phase I goes to Pickett's weakly-coupled metaplaquette scenario.[12] Notice that in this limit the angle φ between metaplaquettes becomes $\pi/2$, instead of 0 or π expected from order-from-disorder ideas. Of course, this phase diagram might be strongly modified by order-parameter fluctuations, but it gives an idea of the model complexity and becomes a starting point for these much more involved calculations.

Notice that the most studied region in connection with the CaV_4O_9 compound ($J_1' \approx J_1$, $J_2 \approx 0.5J_1$) corresponds to a region where several distinct phases merge. On the other hand, Pickett's proposal $J_2 \approx 2J_1$[12] is well inside the phase I. Then, it is of interest to discuss in more detail what happens along the line $J_1' = J_1$ and arbitrary J_2. In Fig. 5 we see the behavior of the energy, with the continuous transition from the short-range Néel order to the incommensurate phase at $J_2 \simeq 0.55J_1$, and then a first-order transition from this last phase to phase I at $J_2 \simeq 0.62J_1$. Fig. 6 shows the corresponding magnetization curve, which indicates a robust magnetic order in phase I and a rather peculiar behavior in the incommensurate phase. In this last phase the magnetization m has an abrupt drop to zero near the transition to the short-range Néel order, which is in agreement with the smooth behavior shown by the energy. However, the incommensurate magnetic vector seems to have a discontinuity before reaching (π, π) (see Fig. 7). Nevertheless, this could be only a problem with the numerical accuracy, since the convergence of the selfconsistent equations becomes more and more difficult near the transition. Another remarkable characteristic of the magnetization curve is the local minimum in the incommensurate phase. Since the behavior of **Q** is smooth across these points, this could indicate that the spins inside the magnetic unit cell rearrange without changing the incommensurate wavevector. Such an explanation is supported by the small discontinuities we observed in the short-range correlations on both sides near the deep local minimum of m. Finally, in Fig. 6 the dashed and full lines in the incommensurate phase give the magnetization of different sublattices. These two sublattices correspond to the zigzagging paths along J_1' and J_2 bonds, in one direction and in the direction perpendicular to it respectively. However, in this case the paths are not disconnected like in the Chain phase, since correlations in J_1 bonds do not vanish. In passing, we note that to obtain this solution from the selfconsistent equations one must allow for different values of the Lagrange multipliers that impose the boson-number restriction on inequivalent sites of the magnetic unit cell.

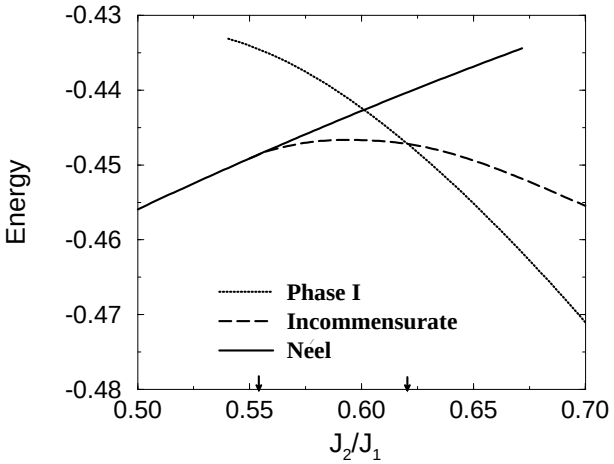

FIG. 5. Ground-state energy along the line $J_1' = J_1$ in parameter space. The arrows at $J_2/J_1 \simeq 0.55$ and 0.62 indicate the points where there are phase transitions.

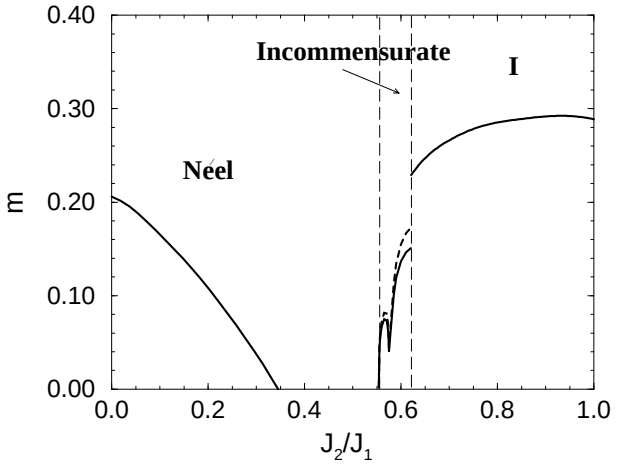

FIG. 6. Magnetization m as a function of J_2/J_1 for $J_1' = J_1$. The full and dashed lines in the incommensurate phase correspond to the magnetization of two different sublattices.

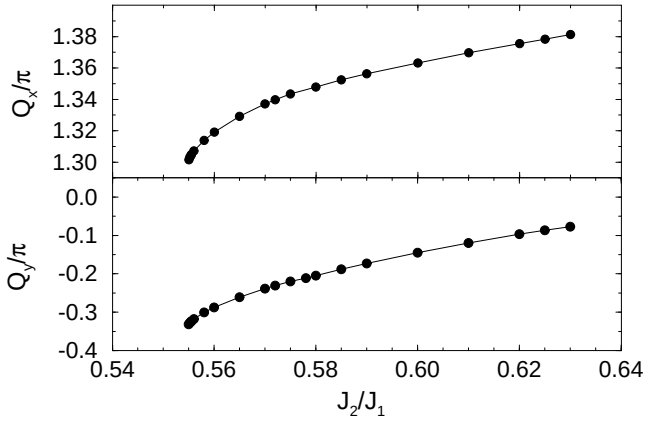

FIG. 7. The magnetic wavevector $\mathbf{Q}/\pi$ in the incommensurate phase as a function of J_2/J_1 for $J_1' = J_1$.

In conclusion, we have determined the general ground-state phase structure of the frustrated Heisenberg model on the CAVO lattice by means of the Schwinger boson mean-field theory. In particular, near the most studied parameter region for the CaV_4O_9 compound we identified several competing phases. Although the relative stability of these phases can be strongly modified by the introduction of Gaussian fluctuations in the order parameters, it is nonetheless quite satisfactory to have a unified picture of the phase diagram at mean-field order. Moreover, it provides a necessary starting point for the more involved one-loop calculations. On the other hand, despite the fact that some of the phases have long-range order –and, consequently, no gap–, the reduced magnetization values suggest that fluctuation corrections might easily destroy the magnetic order and produce the gapped phase observed experimentally (like what happens, for instance, in the $J_1 - J_2$ model on the square lattice[19]). In the absence of frustration, the wavenumber of the lowest energy excitation (corresponding to the singlet-triplet gap in the PRVB scenario) has been predicted from perturbation expansions[3] and variational Monte Carlo[11] to be (π, π), and it shifts to incommensurate wavenumbers when J_2 becomes relatively large. Our results for the Néel, PRVB and I phases indicate also a (π, π) wavector for the lowest excitations, while the incommensurate phase has a $\mathbf{Q}$ that changes with J_2 as shown in Fig. 7. However, recent neutron inelastic scattering data for CaV_4O_9[13] are consistent with $\mathbf{Q} = (0, 0)$, like in a disordered $Q = 0$ phase. Finally, we are currently exploring the possibility of introducing fluctuations in the order parameters, although these are quite involved calculations.

[1] S. Taniguchi *et al.*, J. Phys. Soc. Jpn. **64**, 2758 (1995).
[2] N. Katoh and M. Imada, J. Phys. Soc. Jpn. **64**, 4105 (1995).
[3] M. P. Gelfand *et al.*, Phys. Rev. Lett. **77**, 2794 (1996).
[4] M. Troyer, H. Kontani and K. Ueda, Phys. Rev. Lett. **76**, 3822 (1996).
[5] K. Sano and K. Takano, J. Phys. Soc. Jpn. **65**, 46 (1996); M. Albrecht, F. Mila and D. Poilblanc, Phys. Rev. B **54**, 15 856 (1996).
[6] K. Ueda, H. Kontani, M. Sigrist, and P. A. Lee, Phys. Rev. Lett. **76**, 1932 (1996).
[7] M. Albrecht and F. Mila, Phys. Rev. B **53**, R2945 (1996).
[8] O. A. Starykh *et al.*, Phys. Rev. Lett. **77**, 2558 (1996).
[9] S. R. White, Phys. Rev. Lett. **77**, 3633 (1996).
[10] S. Sachdev and N. Read, Phys. Rev. Lett. **77**, 4800 (1996).
[11] T. Miyazaki and D. Yoshioka, J. Phys. Soc. Jpn. **65**, 2370 (1996).
[12] W. E. Pickett, preprint cond-mat/9704203.
[13] K. Kodama *et al.*, J. Phys. Soc. Jpn. **65**, 1941 (1996); K. Kodama *et al.*, *ibid.*, **66**, 793 (1997).
[14] S. Marini and D. I. Khomskii, preprint cond-mat/9703130.
[15] M. P. Gelfand and R. R. P. Singh, preprint cond-mat/9705122.
[16] N. Katoh and M. Imada, preprint cond-mat/9712051.
[17] Y. Fukumoto, J. Phys. Soc. Jpn. **66**, 2178 (1997).
[18] A. Auerbach and D. Arovas, Phys. Rev. Lett. **61**, 617 (1988); D. Arovas and A. Auerbach, Phys. Rev. B **38**, 316 (1988).
[19] A. E. Trumper, L. O. Manuel, C. J. Gazza and H. A. Ceccatto, Phys. Rev. Lett. **78**, 2216 (1997).
[20] H. A. Ceccatto, C. J. Gazza and A. E. Trumper, Phys. Rev. B **47**, 12 329 (1993).